Retrieval of Raindrop Size Distributions Using Two Doppler Wind Profilers: Model Sensitivity Testing

W. B. MAGUIRE II AND S. K. AVERY

Cooperative Institute for Research in Environmental Science, Department of Electrical and Computer Engineering, University of Colorado, Boulder, Colorado

(Manuscript received 2 August 1993, in final form 30 April 1994)

ABSTRACT

The behavior of precipitation is of great importance in obtaining a better understanding of heat transport estimates and global processes in the atmosphere. This paper discusses improvements in an earlier raindrop size distribution model that utilizes two Doppler wind profilers to obtain accurate measurements of rainfall. A UHF Doppler wind profiler provides a precipitation return while a VHF Doppler wind profiler provides vertical clear-air velocities. The model is tested using simulated data. Sensitivity tests examine the model's ability to estimate rainfall characteristics given typical (noisy) Doppler spectra, and the model's sensitivity to atmospheric parameters. Because it is necessary to estimate pressure, temperature, raindrop temperature, and water vapor pressure at the location of the radar volume, the sensitivity tests examine the effects of errors in the estimates of these parameters. Sensitivity testing of the raindrop size distribution model with simulated data indicates model accuracy and reliability and is necessary in the interpretation of results using real data. Testing shows that the model is very capable at estimating even multiple-peaked drop size distributions from noisy UHF spectra. Sensitivity analyses of atmospheric parameters reveal that model results are quite robust, yielding good accuracy for a wide range of atmospheric parameter estimation errors.

1. Introduction

An understanding of precipitation behavior is crucial in modeling its effects in global atmospheric and climate models. Total water content estimates derived from calculated drop size distributions can be used to obtain estimates of total columnar energy provided via condensation. This measure of total latent heat released may then be useful to the scientific community as an input to atmospheric models or energy budget computations. Satellites are playing an ever-increasing role in the estimation of global precipitation, and a knowledge of the behavior of rainfall (as quantified by the raindrop size distribution and freezing level) will aid satellite calculations of rainfall and water content. Further drop size distribution research will benefit many areas related to environmental science. As a result of inadequate accuracy and data resolution (both temporal and spatial), precipitation behavior as a function of height in the atmosphere is not well understood. Research conducted in determining the raindrop size distribution evolution with height and the 0°C isotherm will result in a better understanding of the parameterization of precipitation in general.

The functional representation of the raindrop size distribution (DSD) has classically been modeled with an exponential. In the four decades since the measurement of raindrop diameters by Marshall and Palmer (1948), exponentials have been used almost exclusively to represent the DSD in all types of rainfall. Varying values of the two exponential parameters are used depending on location and rain intensity.

Recently, there has been evidence to suggest that an exponential representation is inadequate to accurately describe the size distribution of raindrops. Experimentalists have been claiming the merits of the "gamma" distribution to represent the DSD, while theorists have suggested multiple-peaked DSD may evolve in certain circumstances (Valdez and Young 1985; List et al. 1987). Clearly, more studies are required to determine which functions are best suited to represent the DSD in varying types of rainfall.

To study the evolution of the DSD, a more general representation than that of the exponential is desired for the size spectrum. A better DSD representation would be able to approximate multiple-peaked distributions, as well as traditional exponential-like behavior. The work of Currier et al. (1992) pursued the estimation of the DSD using a sum of "modified gamma" functions, which can model multiple peaks as well as be exponential in a limiting case.

The traditional method of estimating rainfall rate from a meteorological radar has been the use of a Z–R (radar reflectivity–rainfall rate) relationship. This power-law function involves two parameters that are

Corresponding author address: W. B. Maguire II, University of Colorado, CIRES, Campus Box 216, Boulder, CO 80309.

experimentally determined. Logically, it is not possible to utilize a Z–R relationship to reasonably determine rainfall rate in varying conditions without an auxiliary measurement device (i.e., rain gauge) for calibration. Even with a calibration device (which may be of questionable accuracy itself), a Z–R relationship is inadequate for anything more than an approximate measurement of rain intensity. By utilizing Doppler wind profilers (and including clear-air vertical velocities), it is possible to more accurately measure rainfall properties.

To accurately measure the DSD using a Doppler wind profiler, it is necessary to know the behavior of the background clear-air vertical velocity. Few calculations have accurately measured and included this effect on the DSD. Unfortunately, it is only occasionally possible to obtain both the precipitation and the clear-air spectral returns from a single-frequency Doppler wind profiler.

Doppler wind profilers operating in the UHF can provide a direct measurement of the (radial) raindrop velocity, although it usually cannot provide information on the updrafts and downdrafts of the clear air (at the same time), which influence drop velocities. Atlas et al. (1973) demonstrated the importance of updrafts and downdrafts and concluded that the vertical clear-air motions must be estimated within about ± 0.25 m s^{-1}. Without the knowledge of the vertical clear-air velocity, Doppler wind profiler estimates of rainfall characteristics are of questionable accuracy.

Gossard et al. (1992) used a UHF Doppler wind profiler to measure rainfall characteristics relying primarily on the Doppler spectral moments, but using a limited number of raw spectra to estimate mean clear-air vertical velocity. As these authors stated, the primary uncertainty in their method involves the separation of the clear-air return from the sometimes overwhelming precipitation return.

A method for retrieving DSDs from a VHF wind profiler was presented by Rajopadhyaya et al. (1994). The method involves separating the clear-air return from the precipitation return, and deconvolving the spectral broadening effects (due to turbulence and beamwidth) to obtain a true fall-speed spectrum. Once again, the method requires a clear separation of the clear-air and precipitation returns in the Doppler spectrum.

Because it is only occasionally possible to obtain both the precipitation and the clear-air spectral returns from a single-frequency Doppler radar, Currier et al. (1992) used two different frequency Doppler wind profilers operated by the National Oceanic and Atmospheric Administration (NOAA) Aeronomy Laboratory. This technique utilized a UHF (915 MHz) Doppler wind profiler to provide precipitation returns and a VHF (50 MHz) Doppler wind profiler to measure the background clear-air motions. In Currier's method, a theoretical DSD is used to calculate a UHF spectral return (with clear-air effects derived from the VHF radar), which is then fit to the actual UHF return spectrum.

Currier conducted only very limited testing of his model on actual data at an experiment in Flatland, Illinois. In addition, Currier's work included no sensitivity analysis using simulated data. The process of incorporating two different frequency radars with the Currier methodology has yet to be thoroughly tested and applied.

Our implementation of the Currier technique, with improvements and alterations, will hereafter be referred to as the "DSD model." The DSD model uses nonlinear least-squares minimization to derive the raindrop size distribution parameters. In Currier's implementation of the Levenberg–Marquardt least-squares algorithm, he did not include the variances of the spectral data points. The spectral point variances are proportional to the spectral power (Doviak and Zrnić 1984; Press et al. 1992); thus the variances vary greatly over the orders-of-magnitude range in the power spectrum values. Inclusion of point variances in the nonlinear least-squares fitting algorithm causes a necessary and significant change. An example of the effect of ignoring spectral point variances will be shown later in section 2d. Our DSD model code takes into account the known variances of the UHF spectral points.

The Currier model code used a summation of gamma functions to represent the drop size distribution. Our DSD model allows the fitting of many types of functions, including gamma, Gaussian, lognormal, and exponential distributions. We have the ability to try many types of DSD representation when fitting to actual data, which will allow us to choose the most accurate yet computationally simple DSD function. For simplicity, we have used Gaussian and exponential DSD functions for our preliminary model sensitivity testing. In reality, a Gaussian does a good job of modeling an exponential: in the limiting case, if the mean becomes large negative ($\mu^2 \gg D^2$), a Gaussian approaches exponential form over the drop range $0 < D < 6$. Therefore when using the model with real data, a sum of Gaussians would be adequately flexible. An exponential DSD does a very poor job of modeling anything other than an exponential.

The DSD model incorporates an automated initialization scheme for each DSD function type, which determines how many functions to fit (resulting in multiple-peaked DSDs) based on a given standard deviation level. This standard deviation level is used by the model to determine if a peak in the power spectrum is significant (compared to the valleys on either side) and warrants an additional DSD function.

Every step of the DSD model code is designed for use in fully automated execution. File input/output and automated initialization are features that are necessary for long, noninteractive model runs with either simulated or real (archived) data. Extensive model runs

are necessary for sensitivity testing, testing against archived data and statistical analyses.

2. Fitting tests

To test the ability of the DSD model's Levenberg–Marquardt nonlinear least-squares algorithm to estimate DSD functions in the presence of noise, "fitting tests" have been executed. Simulated DSDs are used to generate theoretical UHF spectra (including smearing effects such as clear-air turbulence), typical noise behavior is added, and the model then estimates the drop size distribution. Errors in the DSD (between simulated and model calculated) would then be attributable to fitting in the presence of noise. In the following tests, added noise is representative of 52 spectra being averaged. A noisy spectrum is generated by multiplying the value of each spectral point by the negative natural log of a random number between 0 and 1 to obtain power spectrum coefficients with exponential distributions (Zrnić 1975). The variance of each spectral value (periodogram point) is its magnitude, so the average of 52 spectra would result in the standard deviation of a spectral point being $(52)^{-1/2}$ times its value. The DSDs are used to calculate water content as another measure of comparison between the simulated and model-calculated DSD.

In all fitting tests, the clear-air vertical velocity has been set at 0.05 m s^{-1} upward, with a spectral width (Gaussian standard deviation) of 0.55 m s^{-1}, these values would normally be determined from the VHF Doppler wind profiler spectrum. The test values used for the clear-air vertical velocity and spectral width were actual values recorded during an event in 1993 at the NOAA Flatland Atmospheric Observatory in Flatland, Illinois. The DSD model is not sensitive to the clear-air parameters, since our algorithm does not involve any sort of deconvolution to account for the clear-air spectral broadening. All test runs use automated initialization, which is dependent on a significance-level parameter. In the case of fitting Gaussian DSDs, any peak in the power spectrum that is greater than 2.0 standard deviations above spectral valleys on both sides warrants an additional Gaussian DSD function. Gaussian DSDs are initialized by setting the Gaussian mean drop diameter to a value that corresponds to the terminal velocity (including clear-air updrafts or downdrafts) equal to the peak in the Doppler spectrum. The 2.0 standard deviation factor used was determined experimentally, and deemed to provide a good sensitivity to separate peaks while maintaining a low number of false positives (more functions fitted than truly needed). Tests have been run by simulating both exponential and Gaussian single-function DSD representations, and two-function DSDs using a sum of two Gaussians. In some cases, the added noise causes the model to attempt to fit more than the correct number of DSD functions. In the case of fitting to one Gaussian, the model used one Gaussian 95 times out of 100, and two Gaussians 5 times. When fitting to two Gaussians, the model chose to fit two Gaussians 90 times out of 100, and three Gaussians the remaining 10 times.

When the model is allowed to fit to a simulated spectrum that does not contain noise (a control test), the errors are negligibly small. Using a Gaussian DSD, the model-fitted DSD was never in error more than 10^{-4}%; the exponential DSD was within 2.5×10^{-4}%. These errors are a function of the tolerances used for zero finding and integration. The model's sensitivity to drop size is a result of the size dependence of the fall speed for raindrops. The DSD model uses a drop fall-speed relationship from Beard (1977) that is more accurate (and complex) than a simple power-law form.

a. Exponential DSD

To test the model's ability to resolve an exponential DSD in the presence of noise, a simulated exponential DSD was generated using

$$N(D) = N_0 e^{-\lambda D} \tag{1}$$

with $N_0 = 8\,000.0$ m^{-3} mm^{-1}, $\lambda = 2.53$ mm^{-1}, where $N(D)$ is the DSD (m^{-3} mm^{-1}), and D (mm) is raindrop diameter. These values represent a Marshall–Palmer (Marshall and Palmer 1948) distribution for rain of approximately 10 mm h^{-1}. Figure 1 shows a typical exponential simulated-DSD spectrum with a model-derived exponential DSD fit. The top plot in Fig. 2 represents 100 model runs (gray lines) fitting to spectra generated by the exponential DSD (thick black line). The bottom plots in Fig. 2 show histograms of the percentage error of the two exponential parameters between the model fits and the simulated DSD. Because the model allows the fitting of only one exponential, the 2.0 standard deviation threshold used in the automated initialization is irrelevant.

It is evident that the DSD model is quite accurate at estimating the underlying exponential DSD in noisy spectra. The amplitude N_0 of the exponential is usually estimated approximately 5% low, with a spread about the centroid of about ±10%. The exponential parameter λ is estimated much more accurately, with all errors less than 2.5%.

b. Single-Gaussian DSD

As an alternative DSD representation, a simulated Gaussian DSD was generated using

$$N(D) = N_0 e^{-(D-\mu)^2/2\sigma^2}, \tag{2}$$

with $N_0 = 11\,317.1$ m^{-3} mm^{-1}, $\mu = 0.5227$ mm, $\sigma = 0.2936$ mm, where $N(D)$ is the DSD (m^{-3} mm^{-1}), and D (mm) is raindrop diameter. These values were obtained from the Gaussian DSD that results in the model-calculated spectrum shown in Fig. 3, fit to actual data taken from the NOAA Flatland Atmospheric Ob-

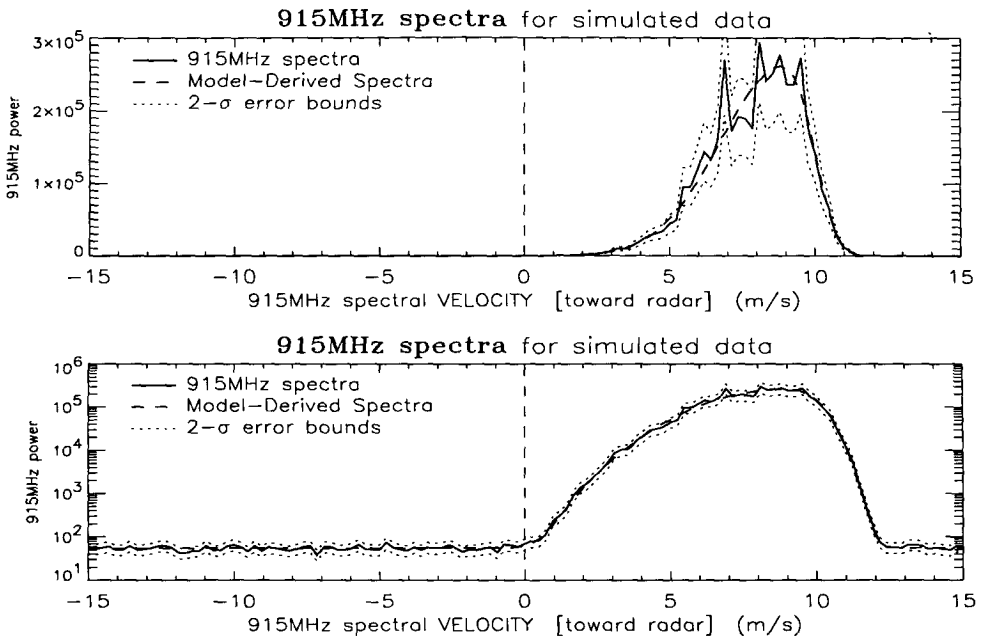

FIG. 1. Sample simulated exponential-DSD UHF spectrum and the resulting model-derived DSD fit plotted on a linear scale (top) and a logarithmic scale (bottom).

servatory. The top plot in Fig. 4 shows the results of 100 model fits (gray lines) to the simulated spectra using the Gaussian DSD (thick black line). Because the model is free to choose any number of Gaussians to represent the DSD, based on the 2.0 standard deviation threshold supplied, occasionally two Gaussians were used (5 times out of 100). A spurious peak is evident at a drop diameter of 0.6 mm that is a result of one of the multiple-Gaussian fits.

Once again, the model is quite accurate at estimating the Gaussian DSD that generated the noisy spectra. As with the exponential DSD, estimation of the amplitude N_0 parameter results in the largest spread of error; the error is centered around 5% low with a spread around the centroid of about ±10%. Both the Gaussian mean and standard deviation are estimated very accurately. In most tests, the estimated Gaussian mean was within ±5% and the standard deviation was usually within ±3% of the value used for the simulated DSD.

c. *Two-Gaussian DSD*

To test the model's ability to resolve a two-peaked DSD in the presence of noise, a simulated two-Gaussian DSD was generated using the sum of two Gaussians [of the form of Eq. (2)]. The first Gaussian is the same as used in the previous section, with an auxiliary Gaussian function added at a mean drop diameter of 3.5 mm. The parameter values of the Gaussians are $N_0 = 11\,317.1$ m^{-3} mm^{-1}, $\mu = 0.5227$ mm, $\sigma = 0.2936$ mm for the first Gaussian, and $N_0 = 0.01$ m^{-3} mm^{-1}, $\mu = 3.5$ mm, $\sigma = 0.3$ mm for the second Gaussian in the sum. Figure 5 shows a sample two-Gaussian simulated-DSD spectrum with the model-derived Gaussian DSD fit. The secondary peak in the spectrum is small enough as to be hardly noticeable in the linear-scale plot. The model is free to choose the number of Gaussians used to fit, and it chose two Gaussians 90 times, and three Gaussians the remaining 10 times. Figure 6 shows the resulting 100 model fits and histograms of the relative parameter errors. Spurious errors can be seen at drop diameters of 1.6 mm and between 2 and 2.6 mm resulting from cases where the third Gaussian used to fit did not disappear.

The errors in the first (primary) Gaussian peak appear consistent with those in the single-Gaussian DSD case. It is evident from the DSD plot and the bottom row of parameter-error histograms that the Gaussian amplitude and standard deviation of the secondary peak have a wider spread of values than those for the primary peak. The second Gaussian peak is more difficult for the model to resolve due to its small amplitude and width. While the DSD model is only able to estimate the Gaussian amplitude and standard deviation of the secondary peak to within about ±50%, it is surprisingly accurate (±3%) at estimating the Gaussian mean.

d. *Effect of spectral point variances*

To test the effect of not including the variances of the periodogram points in the nonlinear least-squares fitting, the DSD model was used to fit (without vari-

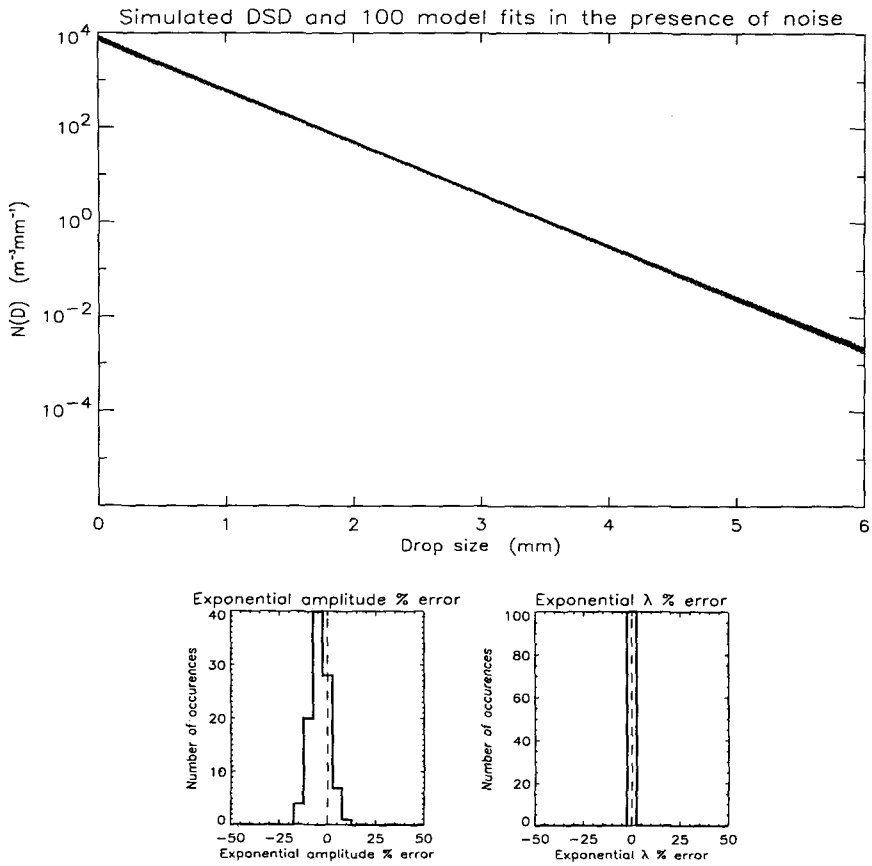

FIG. 2. Model fitting of an exponential DSD to a noisy simulated UHF spectrum generated with an exponential DSD (top), and the exponential parameter errors in fitting to the simulated DSD (bottom).

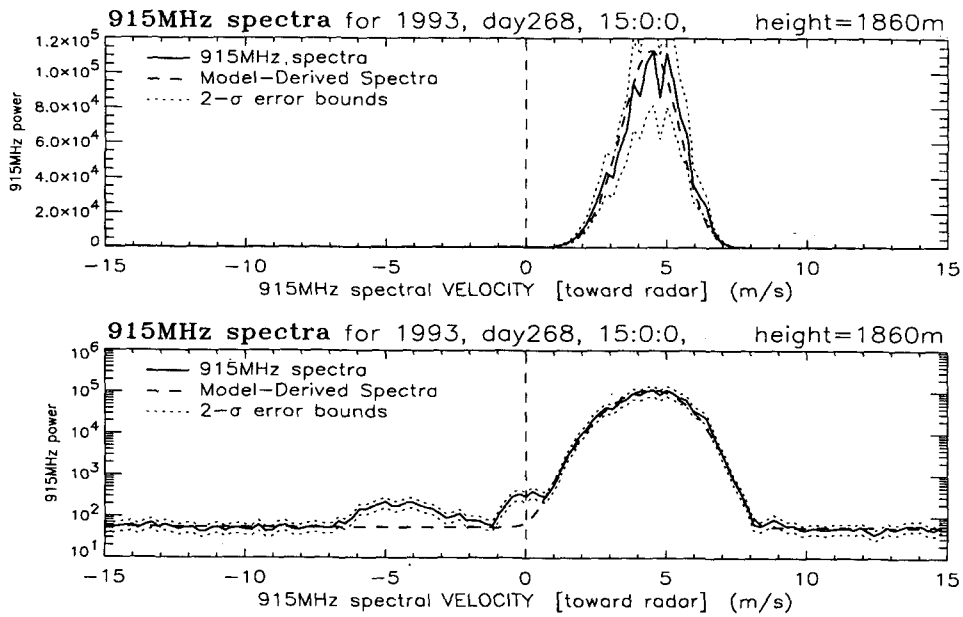

FIG. 3. Actual UHF spectrum (from NOAA Flatland Atmospheric Observatory, Flatland, Illinois) and the resulting model-derived Gaussian DSD fit plotted on a linear scale (top) and a logarithmic scale (bottom).

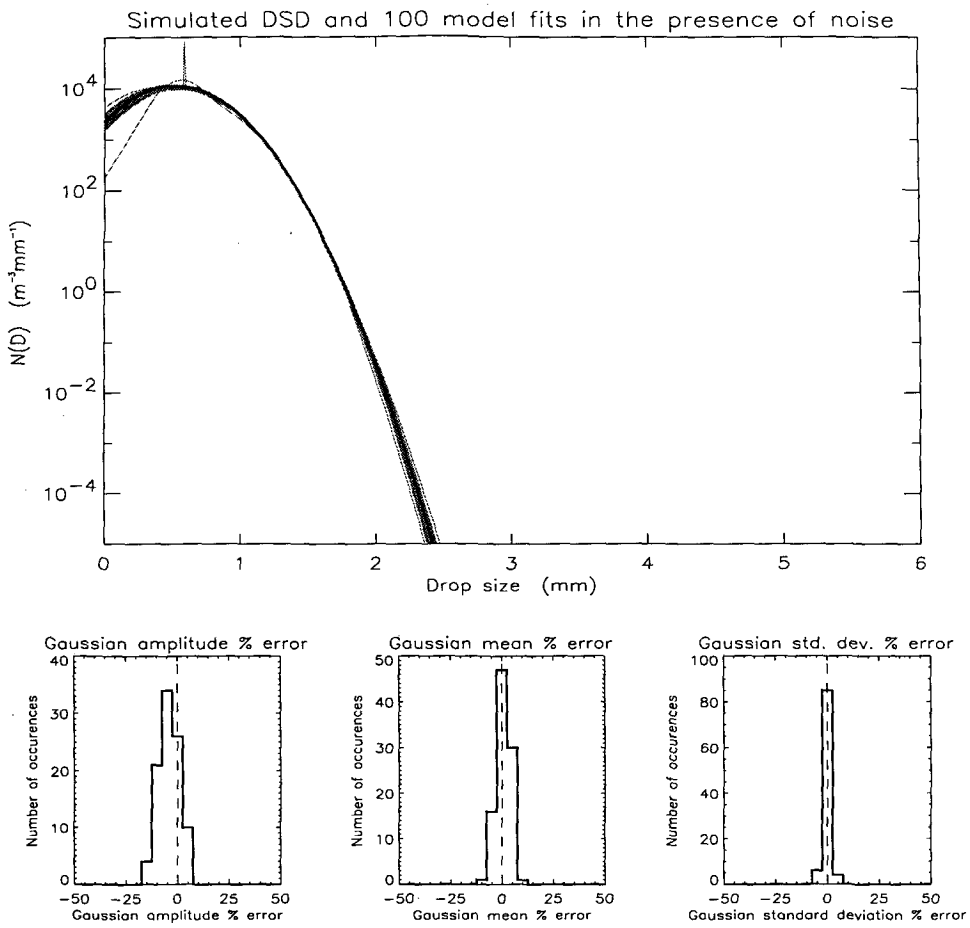

FIG. 4. Model fitting of a Gaussian DSD to a noisy simulated UHF spectrum generated with a Gaussian DSD (top), and the Gaussian parameter errors in fitting to the simulated DSD (bottom).

ances) to noisy spectra with the same simulated DSD as used in the two-Gaussian distribution test. Recall that periodogram point variances are always known: a spectral point's variance is equal to its magnitude (with no averaging in the frequency domain) (Doviak and Zrnić 1984; Press et al. 1992). Because fitting without using spectral point variances is just direct least-squares fitting to the linear spectrum, the model has a very difficult time resolving the small spectral peak (at approximately 9.5 m s^{-1} in Fig. 5). Figure 7 shows the resulting model fits. It is obvious that the fitting is inferior to that in Fig. 6, which includes the spectral point variances. Including the spectral point variances in the least-squares fitting is very close to fitting without point variances to the logarithmic plot of the spectrum. This is easily seen in Fig. 5, because the 2.0 standard deviation error bounds appear to be of uniform width in the logarithmic plot. Use of the spectral point variances in the nonlinear least-squares fitting is essential to resolve features that have small amplitude, and may only be visible in a logarithmic plot.

e. *Water content comparisons*

For each of the above three tests (exponential, single-Gaussian, and two-Gaussian DSD), water content was calculated in each of the 100 model runs. Figure 8 shows a comparison of the three water content error histograms. Figure 8 includes in the single-Gaussian histogram the five cases where two Gaussians were used to fit to a single peak, and the two-Gaussian histogram contains the 10 cases where three Gaussians were used to fit to two peaks.

In all cases the water content errors are about 4% low with a spread around the centroid of about ±6%. These errors are almost identical to the amplitude errors for each of the single DSD functions (Figs. 2 and 4), and the amplitude error of the primary peak for the two-Gaussian DSD (Fig. 6, top row of histograms). It is evident that the amplitude error is the direct cause of the water content error. Evidently the larger errors in the parameters of the secondary Gaussian peak have little effect on the water content errors. This is not surprising. Water content is a third moment of the DSD,

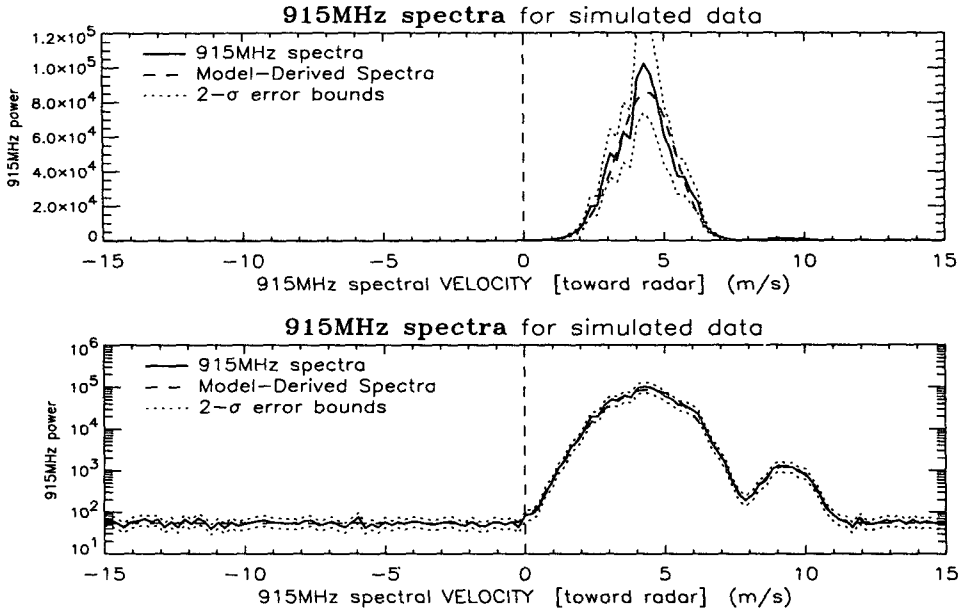

FIG. 5. Sample simulated two-Gaussian DSD UHF spectrum and the resulting model-derived DSD fit plotted on a linear scale (top) and a logarithmic scale (bottom).

so the D^3 contribution of the secondary peak will be a factor of 300 larger than for the primary peak (3.5 mm versus 0.5227 mm), but the secondary peak value is a factor of 1 131 710 lower than the primary peak value (N_0 = 11 317.1 m^{-3} mm^{-1} versus N_0 = 0.01 m^{-3} mm^{-1}).

f. Fitting-test conclusions

As a result of the fitting tests, one can conclude that the model is quite capable of resolving the underlying DSD in the presence of typical noise. The single-function tests involving an exponential and a Gaussian show the model achieving a high degree of accuracy in estimating all the DSD parameters. In the Gaussian tests, an incorrect number of peaks was chosen only a small percentage of the time. If the threshold level were raised to more than 2.0 standard deviations these tests might have shown no incorrect values, but they would be less able to resolve multiple-peaked DSD when the peaks are close together. A value much smaller would frequently cause too many DSD functions to be chosen. The value of 2.0 standard deviation seems a good balance between the extremes. The model's ability to resolve peaks that are very close together is a function of many variables (including spectral width of clear air and magnitudes and widths of the individual DSD functions) and is difficult to test meaningfully. The DSD model's ability in this area will only be seen in testing with real data. Alternative tests for multiple DSD peaks will need to be derived if it is found in real data that DSD functions overlap, thus causing no "valley" between spectral peaks—merely a discontinuity in slope. The number of DSD peaks resolvable is limited, with commonly only 64 to 256 spectral points, it is dangerous to minimize in many-dimensional space. Fitting three Gaussians is already a minimization problem in nine dimensions; good initialization is mandatory! Only experience with real data will determine how many degrees of freedom we will need to adequately represent the raindrop size distribution.

3. Sensitivity to atmospheric parameters

In the application of the model to real data, it is important to know how sensitive the model results are to errors in estimated atmospheric parameters aloft. The DSD model requires estimates of the temperature, pressure, air density, drop temperature, and water vapor pressure at the location of the radar volume. These atmospheric parameters are used to determine drop fall speed (Beard 1977) and radar backscattering cross section (the model does not assume spherical drops; the drops are modeled as oblate spheroids) (Gossard and Strauch 1983). Air density is calculated using pressure, temperature, and water vapor pressure (Wallace and Hobbs 1977) and is therefore not considered an independent parameter for these tests. The following sensitivity tests are needed as indicators of those parameters to which the model is particularly dependent, thus giving a measure to which parameters require accurate estimation.

The sensitivity tests to atmospheric parameters were conducted by simulating the DSD (using exponentials and Gaussians) and generating theoretical spectra without noise. No noise was added because we are not

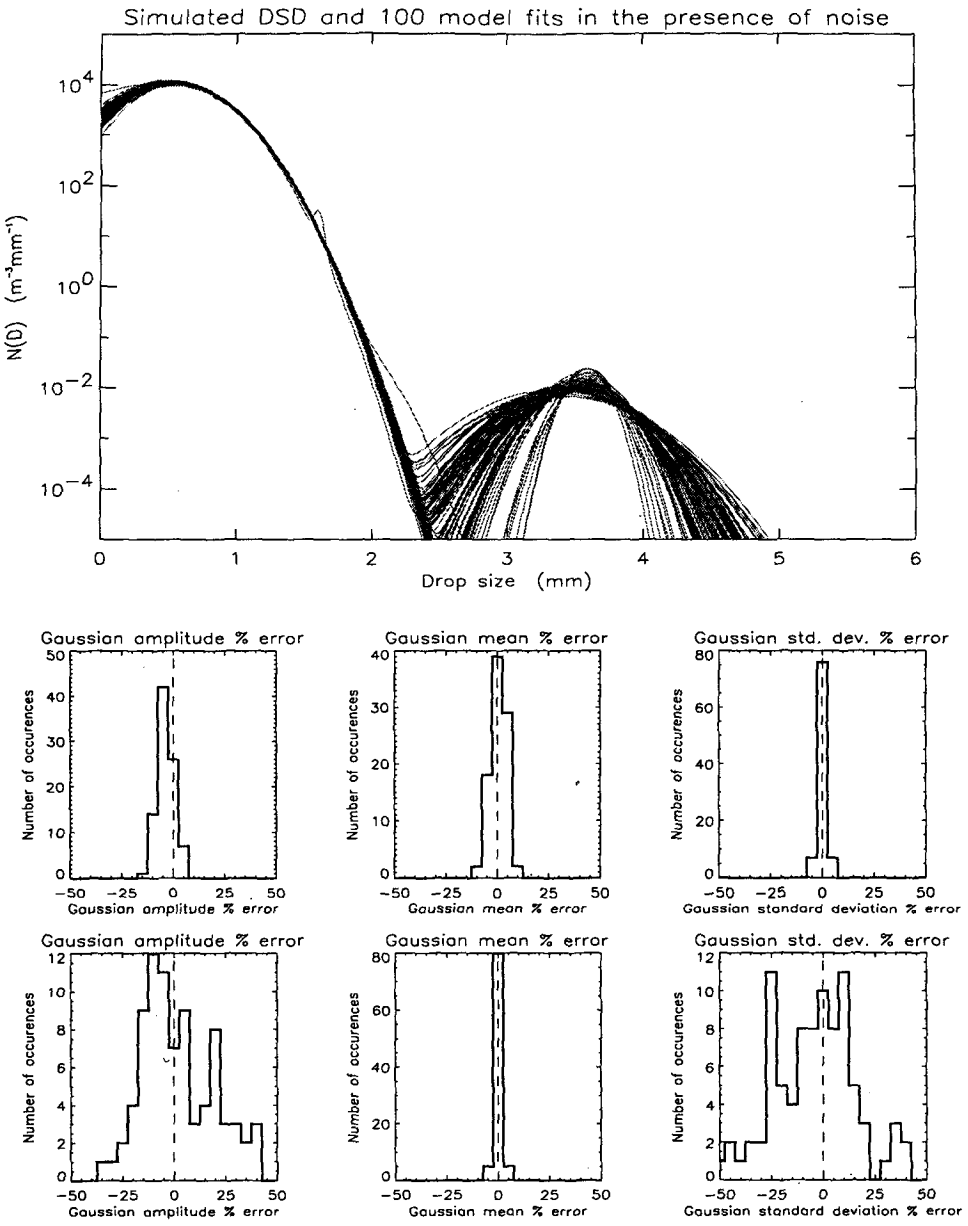

FIG. 6. Model fitting of Gaussian DSD to a noisy simulated UHF spectrum generated with a two-Gaussian DSD (top), and each Gaussian's parameter errors in fitting to the simulated DSD (bottom).

concerned with the least-squares fitting capability, but rather the effect of a change in a single atmospheric parameter. To quantify the sensitivity, a simulated-DSD spectrum was generated with a nominal value of an atmospheric parameter, and the DSD model was allowed to fit to the spectrum using different values of the atmospheric parameter. This process essentially provides a rough partial derivative of the DSD model results with respect to the tested parameter (at the nominal value).

Two techniques are used to illustrate sensitivity to the atmospheric parameters. The first involves plots of the errors in calculated water content, rain rate, and radar reflectivity as a function of the atmospheric parameter. The second method of illustration involves plotting the error in the exponential DSD as a function of drop diameter for two extreme values (above and below the nominal value) of the tested parameter. Errors in the Gaussian DSD were omitted, due to the fact that they become meaninglessly large at many standard deviations from the mean; the exponential is a simpler case for analysis. The first three plots in a figure will indicate the sensitivity of the various moments of the DSD, while

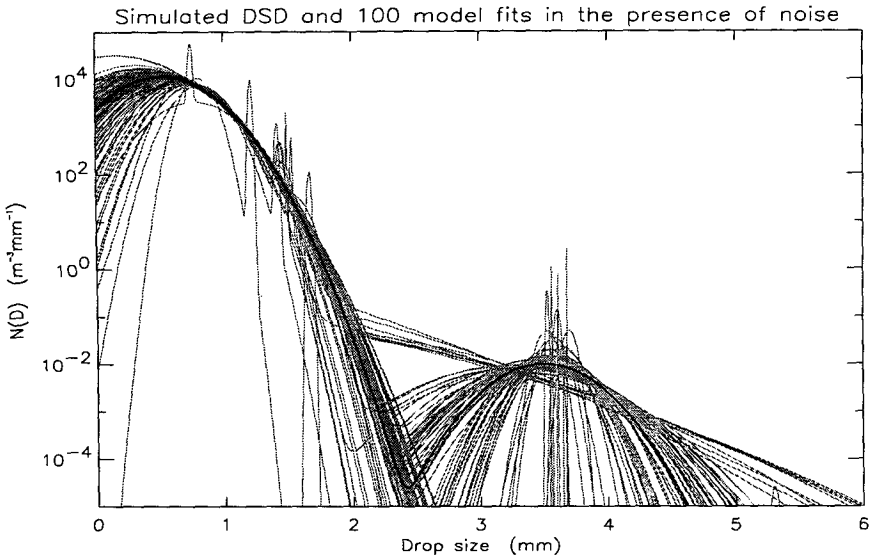

FIG. 7. Model fitting (without point variances) of Gaussian DSD to a noisy simulated UHF spectrum generated with a two-Gaussian DSD.

the fourth indicates the effect on the shape of the (exponential) DSD for errors in atmospheric parameters.

a. Air pressure

Figure 9 (top plot) indicates the DSD model's sensitivity to errors in estimates of air pressure. To test model sensitivity to air pressure, a nominal value of 800 mb was used to generate a spectrum given a simulated DSD (both exponential and Gaussian). The DSD model was then allowed to fit given pressure values from 700 to 900 mb. Figure 9 (top plot) indicates errors in water content calculated from the DSD depend greatly on the shape of the DSD, as the relative errors can be of different signs for the Gaussian and exponential distributions. Using the Gaussian distribution, we see that the error is somewhat linear as a function of pressure, with a negative slope. A 200-mb range in pressure gives rise to a 30% range in water content error. Therefore, we have an order-of-magnitude estimate of water content sensitivity to pressure:

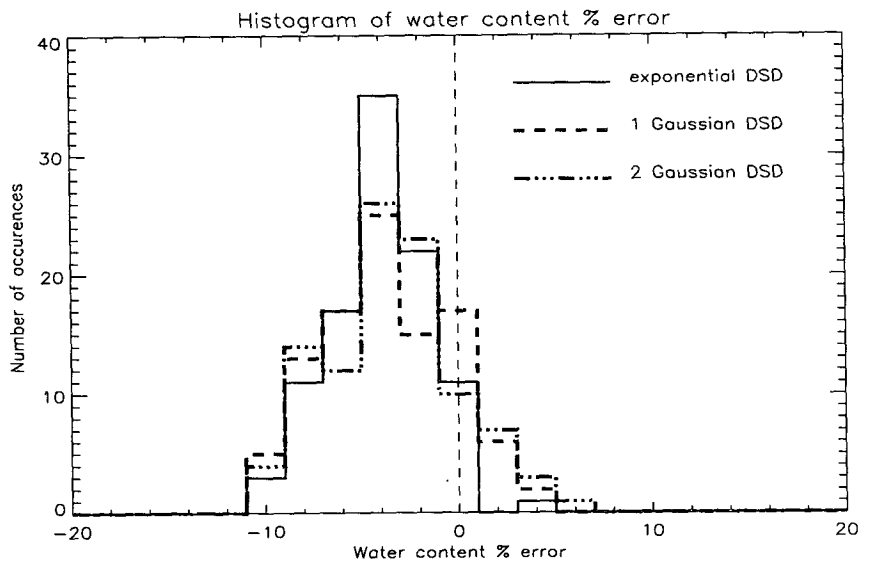

FIG. 8. Histogram of water content errors for the three fitting tests (exponential, one, and two Gaussians).

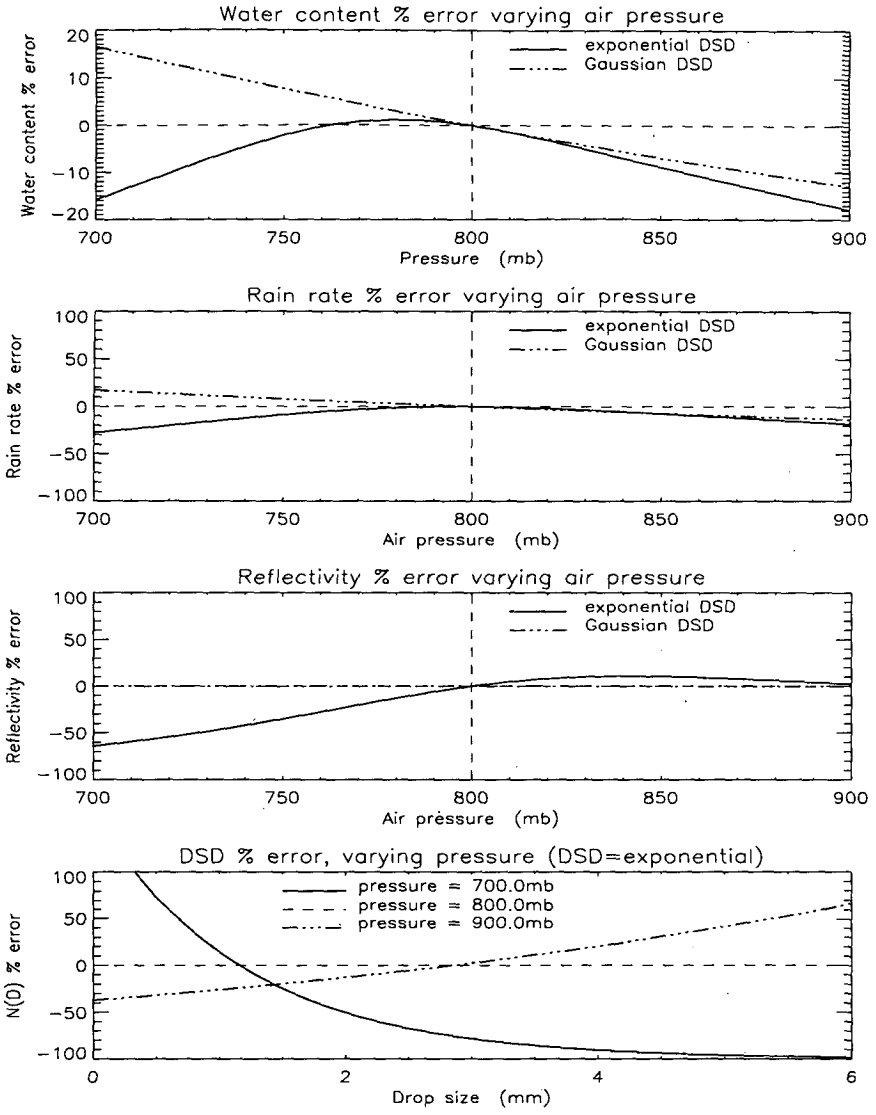

FIG. 9. Calculated water content error (first plot), rain-rate error (second plot), and reflectivity error (third plot) as a function of air pressure; exponential DSD error (fourth plot) for extreme values of air pressure.

a ±20-mb error in pressure causes a ∓3% error in water content. Rain-rate dependence to air pressure is similar to water content, showing 50% range in error for a 200-mb range in pressure. A 20-mb error in pressure causes a ∓5% error in rain rate. Because the signs of the errors differ between the two DSD representations, it is not safe to assume that the water content and rain-rate errors are negatively correlated with pressure (indeed they are positive for part of the exponential DSD regime). Because the Gaussian DSD has another degree of freedom over the exponential, we see from the third plot that a Gaussian DSD shows almost no error in reflectivity. The exponential DSD, however, shows a large relative DSD error at the lowest pressure (on the order of 60%). The bottom plot in Fig. 9 shows that no simple conclusion may be made about the effect of air pressure errors on the DSD as a function of drop diameter. Relative errors in the DSD are shown as a function of drop diameter for the two extremes of 700 and 900 mb. We can see that too low an estimate of pressure causes an excess of smaller drops and a depletion of larger drops. Because the pressure is positively correlated with air density, a decrease in pressure would cause a decrease in air density, which would require smaller drops to match the observed fall speeds. This analysis is consistent with the DSD error plot.

b. Water vapor pressure

Water vapor pressure was tested using a nominal value of 12.5 mb and model fitted with values ranging

from 7.5 to 17.5 mb. Figure 10 (top plot) shows the water content error as a function of water vapor pressure for the exponential and Gaussian DSD. The errors are larger in the case of the Gaussian DSD, and are nearly linear with a positive slope. Using the Gaussian case, we can say that a 10-mb range in vapor pressure gives rise to a 1.2% range in water content error. The order-of-magnitude water content sensitivity to water vapor pressure would then be the following: a ±10-mb error in water vapor pressure causes a ±1% error in water content. Errors in rain rate are very similar, showing a 10-mb error in water vapor pressure causing a ±1.2% error in rain rate. As in the case of air pressure, the Gaussian DSD shows almost no error in reflectivity, while the exponential DSD shows errors of up to 1% at the water vapor pressure extremes. Because water vapor is negatively correlated with air density, the DSD error as a function of drop diameter should be the opposite of air pressure: too low an estimate of water vapor pressure should produce an excess of larger drops and a depletion of smaller drops. This conclusion is consistent with the DSD error graph shown in the bottom plot of Fig. 10.

c. *Air temperature*

Figure 11 illustrates the DSD model's sensitivity to errors in air temperature. To test model sensitivity to

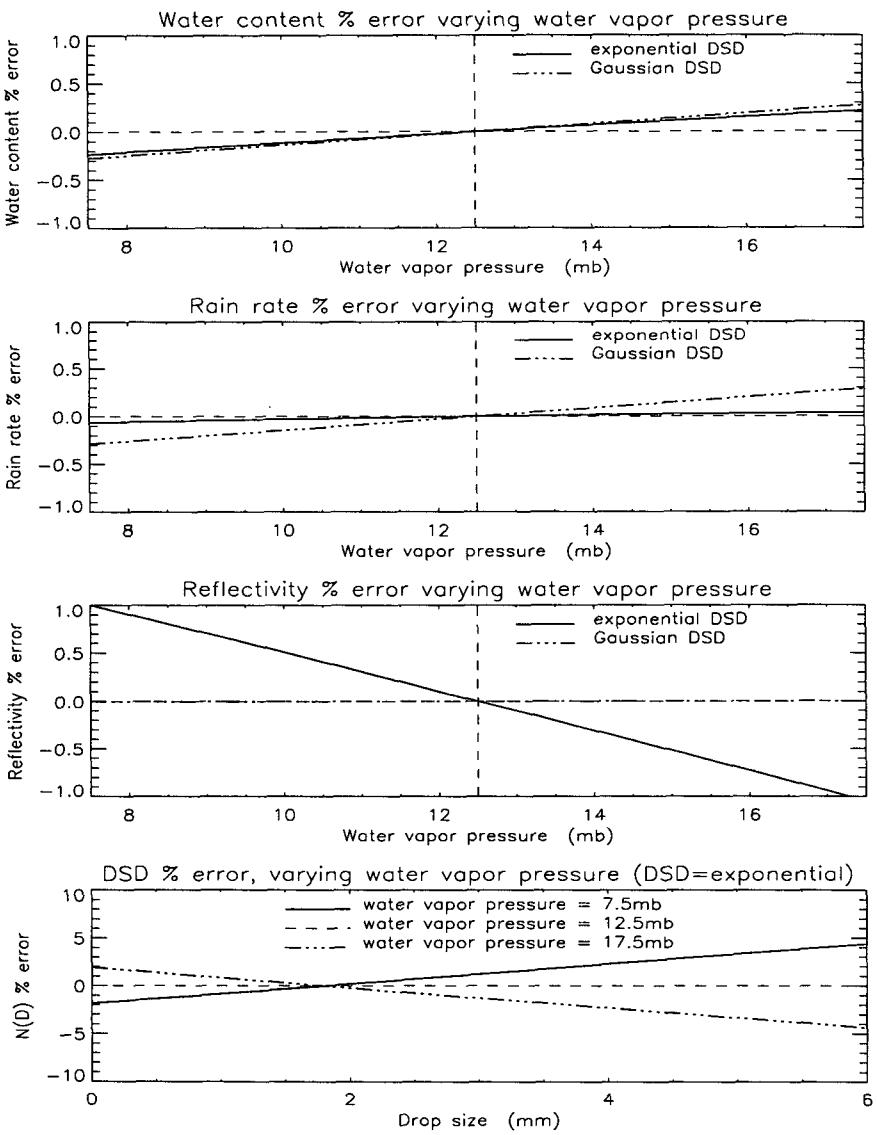

FIG. 10. Calculated water content error (first plot), rain-rate error (second plot), and reflectivity error (third plot) as a function of water vapor pressure; exponential DSD error (fourth plot) for extreme values of water vapor pressure.

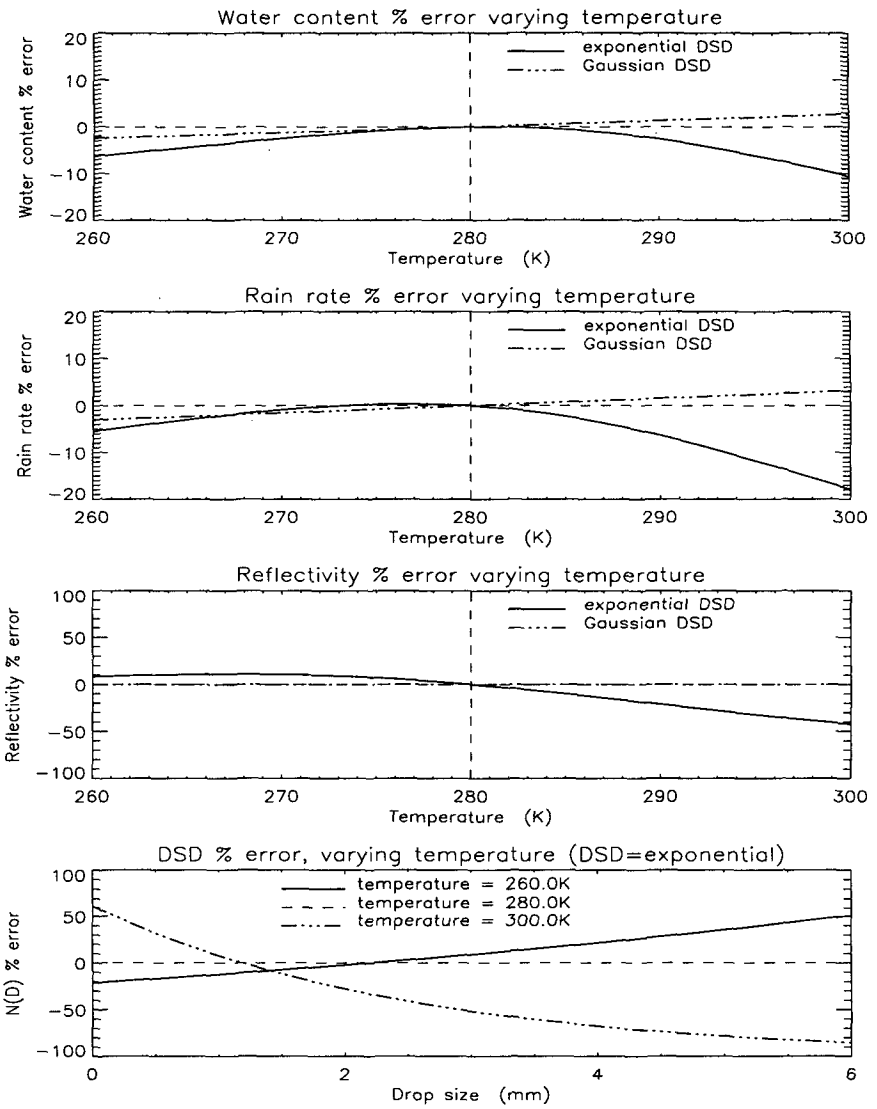

FIG. 11. Calculated water content error (first plot), rain-rate error (second plot), and reflectivity error (third plot) as a function of air temperature; and exponential DSD error (fourth plot) for extreme values of air temperature.

air temperature, simulated spectra were generated using a temperature of 280 K. The model was then used to fit the data using a temperature range from 260 to 300 K. The water content errors vary between the exponential and Gaussian DSD, with the exponential DSD having larger errors, while the Gaussian distribution errors are nearly linear with a positive slope. The top plot of Fig. 11 shows that a 40° range in temperature gives rise to a 10% range in water content error. This result implies that a 10° error in estimating air temperature would give rise to a 3% error in water content. The error results for rain rate are very similar, showing an 18% error for a 40° range in temperature—implying a 10° error in estimating temperature would cause a 5% error in rainfall rate. As for the other atmospheric parameters, the Gaussian DSD does a much better job of matching reflectivity than the exponential; the exponential DSD reflectivity has errors up to 40% at the highest temperature error. Because the temperature affects not only the air density, but also the drop shape, no simple a priori guess may be made of its effect on the DSD as a function of diameter. The bottom graph in Fig. 11 shows that an underestimate in temperature causes an excess of larger drops and a depletion of smaller drops.

d. Drop temperature

Due to the very small model sensitivity to raindrop temperature (because it does not affect fall speed),

sensitivity plots have been omitted. The sensitivity to raindrop temperature was tested using a nominal value of 280 K to simulate data, and fitting was performed over a range from 260 to 300 K. The maximum water content and rain-rate error was approximately 0.5% for the water temperature extremes, while the maximum reflectivity error was approximately 0.003%. The water temperature does not affect fall speed, but does change the dielectric constant and eccentricity of the drop. The maximum error in the DSD values for the exponential DSD were only 1.0% (at the smallest drop diameters).

e. Atmospheric sensitivity-test conclusions

From the model sensitivity analysis of atmospheric parameters, we see that the calculations of water content and rain rate are very robust, even when the parameters are varied greatly. It appears that an error of order 5% can be obtained in water content and rain rate by estimating air pressure to within 20 mb, temperature to within 10 K, and using any reasonable value of raindrop temperature and water vapor pressure. Errors in reflectivity appear to be large for the cases of exponential DSD, while quite small for the Gaussian, showing that additional degrees of freedom in the DSD allow the model to match reflectivity closely. Incorrect estimations of the atmospheric parameters are seen to be a source of DSD error but are not critical enough to be the prime source of inaccuracy. These sensitivity tests will aid in the placement of "error bars" on model results using real data.

4. Conclusions

The DSD model was shown to be quite reliable at extracting the DSD from noisy UHF spectra. The model easily extracted a two-peaked DSD from simulated data, which yields optimism about the ability to research multiple-peaked DSD in real data. The sensitivity tests to atmospheric parameters have shown that the model error is reasonable for a wide range of parameter errors. When the model is applied to real data, these sensitivity tests will be useful in quantifying model error due to inaccuracies in estimated temperatures and pressures.

Acknowledgments. This research has been supported by Grant NA26GP0256-01 from the NOAA Climate and Global Change Program.

REFERENCES

Atlas, D., R. C. Srivastava, and R. S. Sekhon, 1973: Doppler radar characteristics of precipitation at vertical incidence. *Rev. Geophys. Space Phys.*, **11**, 1–35.

Beard, K. V., 1977: Terminal velocity adjustments for cloud and precipitation drops aloft. *J. Atmos. Sci.*, **34**, 1293–1298.

Currier, P. E., S. K. Avery, B. B. Balsley, K. S. Gage, and W. L. Ecklund, 1992: Use of two wind profilers in the estimation of raindrop size distributions. *Geophys. Res. Lett.*, **19**, 1017–1020.

Doviak, R. J., and D. S. Zrnić, 1984: *Doppler Radar and Weather Observations.* Academic Press, 458 pp.

Gossard, E. E., and R. G. Strauch, 1983: *Radar Observation of Clear Air and Clouds.* Elsevier, 280 pp.

——, R. G. Strauch, D. C. Welsh, and S. Y. Matrosov, 1992: Cloud layers, particle identification, and rain-rate profiles from ZRV_f measurements by clear-air Doppler radars. *J. Atmos. Oceanic Technol.*, **9**, 108–119.

List, R., N. R. Donaldson, and R. E. Stewart, 1987: Temporal evolution of drop spectra to collisional equilibrium in steady and pulsating rain. *J. Atmos. Sci.*, **44**, 362–372.

Marshall, J. S., and W. McK. Palmer, 1948: The distribution of raindrops with size. *J. Meteor.*, **5**, 165–166.

Press, W. H., S. A. Teutolsky, W. T. Vetterling, and B. P. Flannery, 1992: *Numerical Recipes in C, The Art of Scientific Computing.* 2d ed. Cambridge University Press, 994 pp.

Rajopadhyaya, D. K., P. T. May, and R. A. Vincent, 1993: A general approach to the retrieval of rain dropsize distributions from VHF wind profiler Doppler spectra: Modeling results. *J. Atmos. Oceanic Technol.*, **8**, 710–717.

Valdez, M. P., and K. C. Young, 1985: Number fluxes in equilibrium raindrop populations: A Markov chain analysis. *J. Atmos. Sci.*, **42**, 1024–1036.

Wallace, J. M., and P. V. Hobbs, 1977: *Atmospheric Science: An Introductory Survey.* Academic Press, 467 pp.

Zrnić, D. S., 1975: Simulation of weatherlike Doppler spectra and signals. *J. Appl. Meteor.*, **14**, 619–620.